

H₂ reduction of CeO₂(111) surfaces via boundary Rh–O mediation

Jun Xu and S.H. Overbury *

Oak Ridge National Laboratory, P.O. Box 2008, Oak Ridge, TN 37831, USA

Received 14 July 2003; revised 9 October 2003; accepted 14 October 2003

Abstract

One of the unique features of cerium oxide is its ability to be reversibly converted into oxygen-deficient structures when it is exposed to a reducing atmosphere. Chemical processes on ceria surfaces serve as gateways in controlling such oxygen transfer. In this work, we have prepared cerium oxide films on which Rh is vapor-deposited and measured the Ce oxidation state following sequential exposure to oxygen and hydrogen. The difference between the fraction of Ce⁴⁺ state of a ceria film resulting from room temperature O₂ exposure and the fraction following sequential H₂ exposure at 400 K was measured for various conditions. Our results show that to achieve an observable reduction by H₂ exposure, O₂ preexposure of the Rh-deposited ceria surface is needed. The H₂ reduction yield increases as the dose of Rh to CeO₂ surface increases. Although this reduction process is observed in as-grown Rh-deposited ceria films, ion sputtering of Rh-dosed ceria surfaces enhances the yield of H₂ reduction. The need of both Rh dose and oxygen preexposure for reduction of ceria by hydrogen suggests that oxygen removal from ceria films is catalyzed by Rh–O. A mechanism is proposed in which Rh–O in intimate contact with ceria transfers hydrogen to ceria lattice oxygen, followed by oxygen removal from the ceria surface through water desorption. Published by Elsevier Inc.

Keywords: Oxide catalysis; Oxygen-storage; Ceria; Reduction; CeO₂(111); Rh; XPS

1. Introduction

Cerium oxide is well known for its oxygen-storage capacity, for which it and ceria-based mixed oxides have found widespread use in automotive emission control systems [1–4]. Reduction and oxidation (redox) cycles in the cerium Ce⁴⁺/Ce³⁺ couple are important for storing or releasing oxygen during air/fuel fluctuations during operation in a three-way catalyst (TWC). Ceria has also been shown to promote steam-reforming and water–gas-shift (WGS) reactions when used as a support for precious metals [5,6]. The promotion effect is believed to be caused by a bifunctional reaction pathway involving a Ce redox cycle. Because of the favorable kinetics for WGS reactions in such catalyst systems it is also of potential interest for use in fuel cells to remove CO in the presence of excess H₂ [7]. It has been reported that deactivation may occur during WGS reaction due to “over” reduction [7,8]. For these applications it is therefore important to understand the processes by which reduction and oxidation of cerium oxide occur.

Redox processes in ceria have been studied for a variety of reductants and oxidants [4,9]. Group VIII metals, such as rhodium and Pt, impregnated into cerium oxide can activate these reactions by adsorbing gaseous species on their surfaces followed by transfer to the ceria support [10,11]. Indeed, much previous work has been done on the reduction of Rh-loaded ceria by CO [12–14] and by H₂ [15–18]. Detailed mechanisms responsible for high-performance oxygen removal are subject to further investigation. In this work, we are interested in chemical species and processes that are associated with the interface between the metal and the cerium oxide since the intimate contact is where hydrogen could be activated to react with lattice oxygen of cerium oxide.

It has been documented that oxidized and reduced ceria powders can be reduced by exposing Rh/CeO_x powders to gaseous H₂ [15–18], even at temperatures lower than 400 K [1,19]. In an effort to elucidate how interaction between CeO₂ and Rh affects catalytic performance, studies of such model catalyst systems conducted in surface science systems are desirable [20,21]. However, no H₂ reduction of CeO₂(111) surfaces has been reported. Our experience and that of others [22] indicate that Rh/CeO₂(111) surfaces cannot be reduced by H₂ exposure at temperatures below 600 K when the surfaces are generated in an ultrahigh vacuum

* Corresponding author.

E-mail address: overburysh@ornl.gov (S.H. Overbury).

(UHV) system. For example, in the present experiments, H_2 exposure in excess of 50 L showed no Ce^{4+} reduction at 400 K. It has been postulated that the reducibility of ceria is related to a specific surface structure [23,24]. For a highly ordered $\text{CeO}_2(111)$ film, the structures that are responsible for H_2 reduction may be lacking. In this paper, we have studied H_2 interaction with Rh deposited onto CeO_2 films using X-ray photoelectron spectroscopy (XPS). Cerium oxide films were reduced by H_2 exposure if and only if Rh/ CeO_2 surfaces were preexposed to gaseous O_2 . The amount of reduction was found to increase with the coverage of Rh on the surface. These results suggest that Rh–O precursors mediate oxygen removal from CeO_2 .

2. Experimental

This work was performed in an UHV system at ORNL, with a base pressure of 1.6×10^{-10} Torr. The system is equipped with Ce and Rh evaporative metal deposition sources, X-ray photoelectron spectroscopy (XPS), a quadrupole mass analyzer (QMA), ion-sputtering gun, and a directed gas doser. Surface composition was characterized by XPS with both Al and Mg anodes. X-ray incidence and electron detection angles are 45° from the sample surface. The binding energy (BE) scale was calibrated using the Ru $3d_{5/2}$ and $3d_{3/2}$ electron peaks at 280.0 and 284.1 eV. The Ce (3d) spectrum was used for monitoring the oxidation state of ceria films [25].

A Ru(0001) substrate disk (10 mm diameter) was mounted on two heating tungsten wires (0.25 mm in diameter), with which the sample can be heated with minimal heating of the sample holder. The Ru surface was cleaned by 1 keV Ar^+ ion followed by annealing at 900 K for 2 min. CeO_2 films were grown in situ using the following steps. Ce was deposited onto the Ru(0001) surface by heating a Ta foil envelope containing a strip of Ce metal. Ce vapor was confirmed by measuring mass 140 using QMA before exposing to the substrate. Oxygen was introduced into the chamber to 3.0×10^{-7} Torr at the start of Ce dosing. The substrate temperature was maintained at 700 K during CeO_2 growth [26]. Ce deposition times of 5 to 20 min were used depending on the desired thickness of ceria film, after which the Ce evaporator was turned off while the O_2 pressure maintained at 2.0×10^{-7} Torr. The substrate temperature was increased to 900 K for 30 s and then cooled down to 600 K at a rate of approximately 2 K/s. Then the oxygen was evacuated while the surface cooled to room temperature. In previously reported experiments we have demonstrated that growth under these conditions leads to films which primarily have a (111) orientation [26], although in the present system confirmation by LEED was not possible. To obtain a reduced ceria film the oxygen pressure was decreased to less than 1.0×10^{-7} Torr during the Ce deposition or the ceria surface could be sputter-reduced.

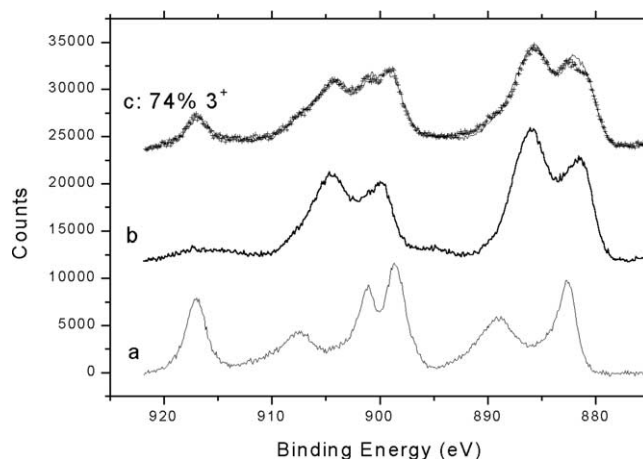


Fig. 1. Ce 3d XPS spectra from cerium oxide in three different oxidation states: (a) fully oxidized surface assumed 100% Ce^{4+} , (b) highly reduced surface, assumed 100% Ce^{3+} , and (c) an intermediate oxidation state determined by curve fitting to 74% Ce^{3+} . In curve (c) the crosses correspond to the data and the solid curve corresponds to the fitted linear superposition of 0.26 times curve (a) and 0.74 times curve (b). All curves were background-subtracted and normalized to equal integrated intensity. Curves (b) and (c) are offset vertically.

XPS measurements of the films generated by this procedure showed a highly oxidized ceria, shown in Fig. 1a after applying an integral background subtraction procedure. This spectrum exhibits an intense, sharp peak at 918 eV and is assumed to have all of the Ce in the Ce^{4+} state. Based on the attenuation of the integrated Ru (3d) XPS peak intensity, typically around 80%, the thickness of the CeO_2 layer was estimated to be a few nanometers. Highly reduced ceria films were produced by ion sputtering or by reducing O_2 pressure during Ce deposition, leading to substantial changes in the Ce 3d spectrum as shown in Fig. 1b [25]. The spectrum in Fig. 1b indicates, a complete loss of the 918 eV peak, a signature of a highly reduced ceria associated with complete conversion of Ce^{4+} to Ce^{3+} . The extent of reduction of any ceria film of intermediate oxidation state was obtained by comparison to these two spectra and using the following curve-fitting procedure. Spectra of the intermediate film and of the fully oxidized and highly reduced spectra were corrected to remove the secondary electron tail using an integrated background procedure and then normalized to unit integrated intensity. A simple linear combination of the highly reduced and the fully oxidized spectra was optimized to give the best fit to the intermediate with a single parameter, the fraction of the fully oxidized spectrum. A typical spectrum from a film of intermediate oxidation state is shown in Fig. 1c along with the fitting results.

Rhodium was deposited onto the ceria films at 300 K using a Rh wire wrapped around a 0.25-mm W filament. After deposition the Rh/ CeO_x film was heated to 900 K for 30 s. Previous work suggests that the deposited Rh does not grow in a layer-by-layer fashion, but aggregates into islands [26,27]. Our measurements indicate that the Rh 3d intensity decreases and Ce increases after 900 K flash

for 30 s, which suggests that Rh further aggregates upon annealing, consistent with Volmer–Weber growth model [28]. XPS measurements showed that deposition of Rh causes an apparent slight reduction of fully oxidized CeO_2 to CeO_x ($x = 1.995$ to 1.975) when Rh is deposited.

H_2 exposure was performed through a doser tube with one open end, approximately the size of the substrate surface, closely facing the substrate surface. Gas flow into the tube is limited by a laser-drilled effusion hole with about $5\text{ }\mu\text{m}$ diameter through a VCR blank gasket. H_2 was introduced through the tube by setting H_2 pressure behind the aperture at 0.4 Torr, fixing the dose rate. Total dose was adjusted by varying the dose time. For a given dose, H_2 emitted from the aperture was varied in range of $0\text{--}9 \times 10^{16}$ molecules, assumed to impinge once on the front surface of the sample with surface area of 0.8 cm^2 . O_2 exposure was performed by backfilling the UHV.

3. Results

Fig. 2 shows XPS spectra of Ce 3d electrons for (a) fully oxidized CeO_2 surface, (b) H_2 exposure to the surface in (a), (c) Rh-doped CeO_2 surface, and (d) H_2 exposure to the Rh/ CeO_2 surface. As shown in Fig. 2a and 2b, exposure of a fully oxidized CeO_2 surface to 3.3×10^{16} molecules of H_2 at 600 K does not induce reduction. About a monolayer equivalent of Rh was deposited onto the surface of a fully oxidized ceria film, followed by annealing at 900 K for 30 s. The fraction of Ce^{4+} state is decreased from 100% to approximately 96% as a result of the Rh deposition. The percentage of Ce^{4+} state was not changed after the same amount of H_2 exposure to the Rh/ CeO_x surface at 600 K. These results are in contrast to Rh-loaded ceria powders where the ceria is dramatically reduced by presence of high-pressure H_2 [1,15–19].

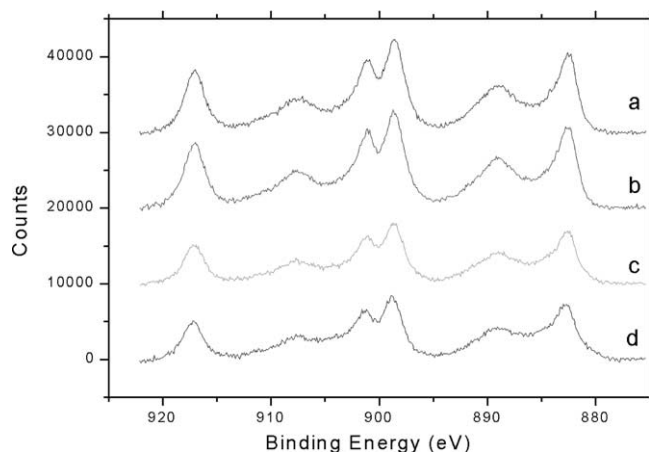


Fig. 2. Ce 3d XPS spectra are shown for (a) an as-grown oxidized CeO_2 surface, (b) surface in (a) after exposure of the surface to 3.3×10^{16} H_2 molecules at $T = 600\text{ K}$, (c) a CeO_2 surface deposited with 1.1×10^{15} Rh atoms/ cm^2 , and (d) the surface in (c) following exposure of the surface to 3.1×10^{16} H_2 molecules at 600 K.

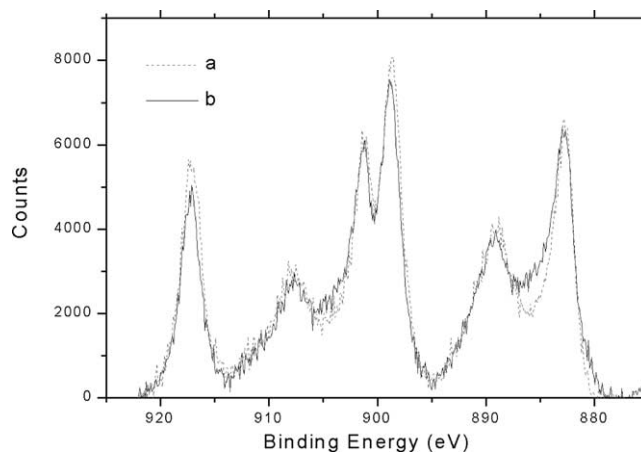


Fig. 3. Ce 3d XPS spectra for $\text{O}_2\text{--H}_2$ cycle for a flat as-grown Rh-deposited ceria film, (a) O_2 exposure, and (b) H_2 exposure.

Predosing the surface with oxygen enhances the reduction of the ceria as demonstrated by the experiments in Fig. 3. Rh-loaded CeO_x surface, 96% oxidized or $x = 1.98$, was exposed to O_2 at a pressure of 2.0×10^{-7} Torr for 10 min at room temperature. The surface was 99% Ce^{4+} after O_2 exposure, as shown in Fig. 3a. Then the surface was exposed to about 6×10^{16} H_2 molecules at 400 K and the proportion of Ce^{4+} state was reduced to be 88%, as shown in Fig. 3b. Such a reduction of Ce must be related to the O_2 preexposure because everything else was the same as for the case without the O_2 preexposure where no reduction was observed. This experiment suggests that the oxygen is mediating the reduction of the ceria by hydrogen.

In a separate experiment, the Rh-loaded CeO_x surface was preconditioned by Ar ion sputtering before initiating the $\text{O}_2\text{--H}_2$ exposure cycle described above. The sputtering dose of $5\text{ }\mu\text{A}$ for 1.5 min caused reduction leaving a surface that is 57% oxidized. This sputter-reduced surface was exposed to O_2 at a pressure of 3.0×10^{-7} Torr for 10 min at room temperature. The surface is 83% oxidized after this oxygen exposure, as shown in Fig. 4a. Sequentially the surface was

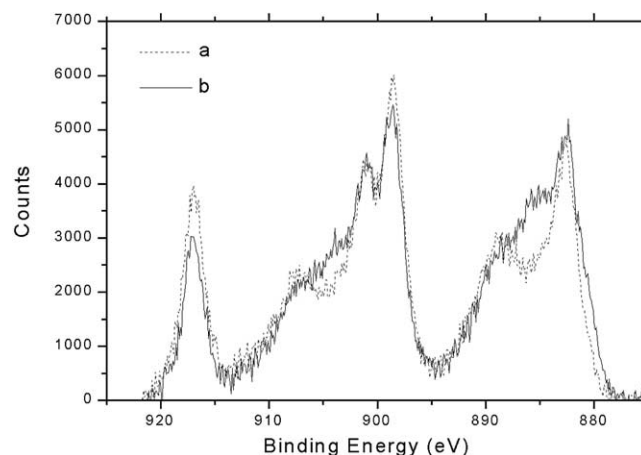


Fig. 4. Ce 3d XPS spectra for $\text{O}_2\text{--H}_2$ cycle for Rh-deposited ceria films that were sputtered before the cycle, (a) O_2 exposure, (b) H_2 exposure.

exposed to 8.7×10^{16} H₂ at 400 K, causing reduction to 64% oxidized as shown in Fig. 4b. The difference between the percentage of Ce⁴⁺ of the ceria film resulting from the O₂ exposure and the percentage following the sequential H₂ exposure is typically 20%, a bigger difference than the 10% difference which is typically seen for the unspattered surface. Clearly, presputtering of the Rh-loaded CeO_x surface further enhances reduction of CeO_x during the O₂–H₂ cycle.

It is interesting to note that the Rh 3d electron peak position, measured by XPS, is consistently shifted by the presence of oxygen. Before O₂ exposure, the XPS Rh 3d_{1/2} peak is at a BE of 307.0 eV, thereafter referred as Rh metal state. After O₂ exposure, the Rh peak is shifted to a higher BE by 0.3 eV, indicating chemisorption of oxygen on the Rh. The oxygen exposure is not sufficient to completely oxidize the Rh particles, since complete oxidation should result in a 1.0 to 1.3 eV shift in the peak position depending upon Rh oxidation state [29,30]. After the subsequent H₂ exposure, the peak shifts back to the position of the Rh metal state, indicating removal of oxygen from the surface of the Rh particles.

Fig. 5 shows the extent of Ce⁴⁺ reduction induced by the O₂–H₂ reduction cycle as a function of the amount of Rh on the surface. A CeO₂ surface was dosed with Rh for a certain deposition time, followed by the O₂–H₂ exposure cycle. In this case, the surface was not sputtered. After reduction by extended H₂ exposure at 400 K the fraction of Ce⁴⁺ decreases compared to its value after the prior O₂ treatment at 300 K (1×10^{-7} Torr for 10 min). This decrease is plotted in Fig. 5 as a function of Rh dose. The amount of deposited Rh was estimated from the ratio of integrated Rh 3d peak intensity after a certain disposition time to the (Ru 3d) intensity measured for the clean Ru substrate. (The intensity of the Ru 3d peaks approximates the intensity of the Rh 3d peaks for a thick Rh film to within about 12% [31].) It is seen in Fig. 5, that increasing Rh deposition causes an increase in the oxygen mediated reduction of ceria up to about

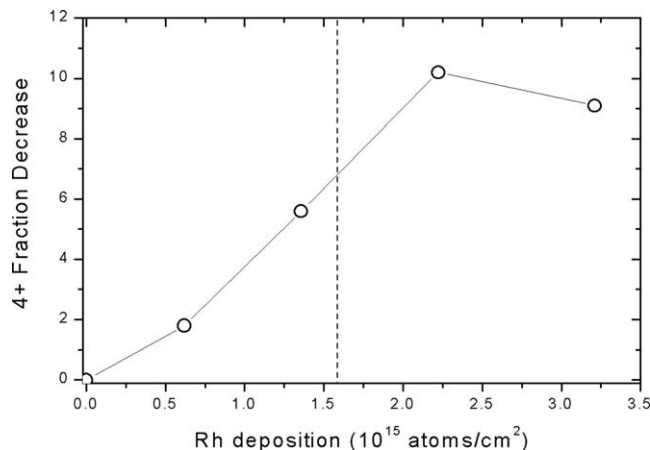


Fig. 5. Reduction of Ce⁴⁺ resulting from H₂–O₂ cycles as a function of Rh load.

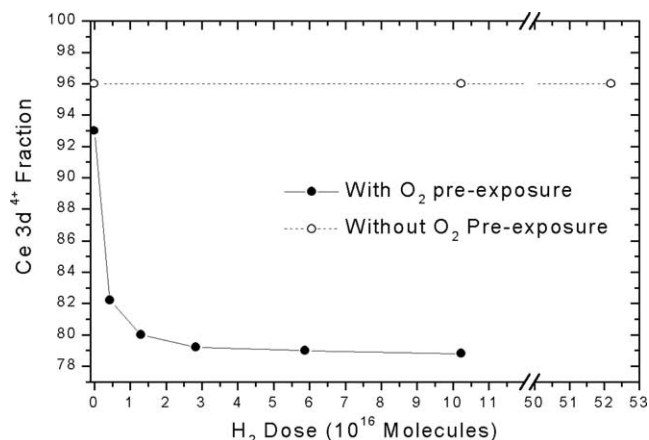


Fig. 6. Change of Ce⁴⁺ fraction from that for O₂-preconditioned Rh/CeO_x surface as a function of H₂ exposure. Exposure is expressed as the amount of H₂ flowing through the dosing aperture.

2×10^{15} atoms/cm² where it saturates or even decreases. Such an increase in the low deposition range may be related to an increase in the numbers of boundary sites between the Rh islands and the ceria, which are necessary for the oxygen-mediated reduction.

Fig. 6 shows reduction of the Ce⁴⁺ state as a function of H₂ exposing time. The CeO_x surface was loaded with Rh estimated to be 1.2×10^{15} atoms. The surface was sputtered by Ar ions and then exposed to 2×10^{-7} Torr or O₂ at room temperature for 10 min. Sequentially the surface was exposed to H₂ doser for variable times, corresponding to the exposures shown in the figure. The majority of the reduction occurs with a dose of less than the first 10^{16} molecules of H₂. In the absence of the oxygen pre-dose, no reduction occurs for H₂ doses as large as 5×10^{17} .

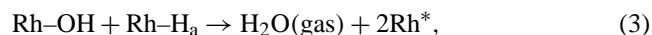
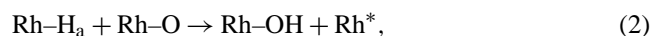
4. Discussion

Experimental results show that to reduce Rh-deposited ceria films by H₂ exposure, O₂ preexposure is needed. In this two-stage process, the amount of reduction increases with the dose of Rh and as a function of H₂ exposure time. Such a reduction by the two-stage O₂–H₂ cycle is enhanced for by presputtering of the Rh-loaded ceria surfaces. These results suggest that formation of an Rh–O species on Rh-loaded CeO_x(111) surfaces is necessarily an intermediate step for ceria film reduction when the surfaces are exposed to gaseous H₂. The following steps are postulated to describe such a Rh–O-mediated process.

Stage 1: During the first stage of the cycle, it is expected that O₂ exposure of a Rh-loaded CeO_x surface at room temperature forms chemisorbed oxygen on surface and boundaries of the Rh islands, (Rh–O) and (Rh–O)_B, as well as induces oxidation of the ceria. It has been reported that molecular oxygen, weakly bound peroxide, or superoxide, is formed by O₂ chemisorption on reduced ceria [32,33]. However, these cannot play a role in the present oxygen-mediated

reduction since they do not seem to persist up to the temperature where we have performed the subsequent reductions and they do not occur on fully oxidized ceria [32,33]. It may also be possible that oxygen induces increased dispersion of the Rh. Such redispersion cannot alone be responsible for the oxygen-induced reduction since even prior to the oxygen exposure the Rh is well dispersed, but hydrogen reduction does not occur.

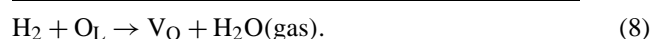
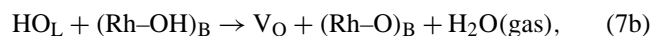
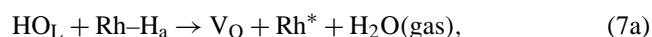
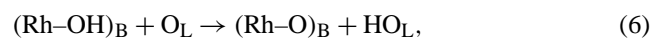
Stage 2a: During the second stage of the cycle, H₂ exposure on the O-covered Rh islands results in water formation by the following reactions:



In the above, empty sites on the Rh islands are indicated as Rh*. The presence of ceria is expected to have little effect on these steps. There is considerable evidence for this Langmuir–Hinshelwood mechanism on Rh(111) and Rh(100) single-crystal surfaces [34–36]. Early work by Yates et al. indicates that on Rh(111), preadsorption of oxygen does not eliminate subsequent adsorption of H₂ and reaction to form water at 335 K, especially if the oxygen overlayer is well ordered [34]. Their isotope studies provide evidence that water formation occurs by the Langmuir–Hinshelwood mechanism in steps (1)–(3). Similarly, significant amounts of H₂ can be adsorbed on ordered oxygen overlayers on Rh(100) at 200 K [36]. Water and H₂ is desorbed near room temperature in subsequent TPD, removing O from the Rh surface. The formation of hydroxyls, step (2), is further supported by detection of OH by HREELS on Rh(100) [35].

In our experiments the shift in the Rh 3d XPS peak provides evidence that oxygen removal is induced by the subsequent hydrogen exposure. After O₂ exposure, the Rh 3d-binding energy is shifted 0.3 eV due to the chemisorption of oxygen and then after sequential H₂ exposure, the binding energy returns to the Rh metal state. It is noted that these reactions occurring on the Rh islands do not affect H₂ reduction of the ceria film.

Stage 2b: In the boundary sites between the oxygen-covered Rh islands and the ceria support, (Rh–O)_B reacts with H₂ and transfers H to ceria, as described by the following steps:



In the above, O_L refers to an oxygen anion in the cerium oxide lattice, and V_O is a vacancy generated on the cerium oxide. As indicated in Eq. (5), Rh–O at the boundary, (Rh–O)_B, forms rhodium hydroxyl, (Rh–OH)_B, with adsorbed hydrogen resulting from H₂ exposure. Hydrogen transfer produces hydroxyl, HO_L, at the lattice oxygen of ceria. This transfer in step (6) occurs in competition with water formation on Rh in step (3). A subsequent transfer of H_a to the hydroxyl on the ceria occurs, (7a), and then desorption of water leads to the formation of a ceria oxygen vacancy. A possibly competing process, step (7b), is the transfer of H from (Rh–OH)_B to the ceria hydroxyl, HO_L. Note that although hydroxyls are formed on the ceria, it is assumed that these do not react with each other to form water at 400 K. This assumption is based upon previous work that showed that hydroxyls on ceria react to evolve only H₂ and only above 500 K [21]. Reduction of Ce⁴⁺ measured by XPS is proof of generation of V_O. Reaction (8) is the total result of this reduction cycle, which is mediated by boundary Rh–O.

The oxygen mediation as described above is specific to H₂ reduction since it involves H transfer through hydroxyls. It is possible that a similar mechanism could occur for reduction by CO, involving transfer of oxygen or of CO between Rh boundary and cerium oxide. Additional experiments would be required to determine if there is evidence for such a pathway.

Enhancement of the H₂ reduction of CeO_x film by ion sputtering suggests that sputtering induces an increase in the number of boundary sites. This may occur because sputtering further disperses the Rh atoms. Of course an increased amount of boundary sites increases the yield of step (8).

Our previous work has shown that hydroxyls, formed by water adsorption onto a reduced and Rh-loaded cerium oxide, decompose above 500 K during TPD to form hydrogen instead of water [21]. The result is oxidation of the ceria. This seemingly contradicts the reduction of ceria and the water desorption described in steps (7a) and (7b). However, in those water adsorption experiments, neither adsorbed hydrogen atoms nor hydroxyls on Rh were available. According to step (7), formation of water on ceria requires both oxygen-mediated formation of hydroxyls on ceria and their reaction with hydrogen atoms or hydroxyls adsorbed at the Rh boundaries. Desorption of this water, carrying away a lattice oxygen anion, results in reduction of the cerium oxide.

This work therefore provides an explanation for why cerium oxide single-crystal surfaces and films, even when loaded with Rh, are not readily reduced by hydrogen under UHV conditions. In the absence of Rh, there is no surface for H₂ to adsorb and dissociate upon. The presence of Rh provides a source of atomic hydrogen available for reduction, but evidently hydrogen transfer from the Rh to the ceria is not facile. Chemisorption of oxygen on the Rh oxygen or at the Rh boundaries provides an alternate pathway to transfer H to the ceria that evidently has a lower activation barrier.

These results have various implications. The occurrence of the oxygen-mediated reduction implies that isotopically labeled oxygen could be exchanged into the surface of Rh-loaded and fully oxidized ceria surface by exposure to a mixture of hydrogen and oxygen. Hydrogen would reduce the ceria through oxygen-mediated reduction, which would then be followed by reoxidation by the isotopically labeled oxygen, a facile process which occurs even in the absence of Rh. Such exchange would not be expected for exposure to the oxygen alone. Another prediction is that following the formation of OH on ceria by other means, such as exposure to water, reduction should occur by subsequent exposure to hydrogen. Such reduction should be observable by H₂O desorption or direct measurement of the Ce³⁺.

Although the oxygen-mediated reduction is postulated to occur at the boundaries of the Rh islands, reduction is not limited to those sites. The amount of reduction measured by XPS implies that 10–20% of the top several layers of the cerium oxide are reduced. Our experiments show that observable oxygen migration occurs at temperatures as low as 300 K. Migration of oxygen anions and vacancies could lead to reduction throughout a zone surrounding the Rh islands. Since oxygen on the Rh boundary is not consumed during the oxygen-mediated transfer then a considerable amount of H can be transferred to the ceria support leading to substantial reduction. At 400 K, the temperature at which the O₂–H₂ cycles were run, hydroxyls formed on ceria do not react to evolve H₂O or H₂ [21], thereby preventing loss of the HO_L reactant necessary for step (7).

The oxygen-mediated mechanism provides a means by which reduction of ceria can be enhanced on highly oriented cerium oxide films prepared and loaded with Rh under UHV conditions. Under such conditions oxygen can be routinely excluded from the Rh which is deposited onto the smooth cerium oxide film in oxygen-free conditions, leading to surfaces that are difficult to reduce by H₂ alone. Previously, the more facile surface reduction of Rh-loaded polycrystalline or of highly dispersed cerium oxide has been attributed to “structural” differences in the cerium oxide [23]. It may be that these structural differences involve oxygen at the Rh boundaries which facilitate hydrogen transfer from the Rh. In highly dispersed ceria catalysts, loaded with Rh by wet impregnation, it may be difficult to exclude all oxygen from the surface or boundaries of Rh particles, especially if conditions cycle between reducing and oxidizing. Such boundary oxygen may therefore be an important, but previously unsuspected, intermediate in practical ceria-supported precious metal catalysts under realistic conditions.

5. Conclusion

The extent of reduction caused by exposure to H₂ has been studied for Rh-loaded cerium oxide films. The relative amounts of Ce⁴⁺ and Ce³⁺ are determined quantitatively by XPS and used as a measure of the progress and extent of re-

duction. It is found that H₂ is ineffective in reducing ceria or Rh-dosed ceria. However preexposure to oxygen mediates the reduction during a subsequent exposure to hydrogen. The amount of reduction resulting from the O₂–H₂ exposure cycle increases as the dose of Rh on the CeO₂ surface increases. Ion sputtering of the Rh/ceria surface enhances the amounts of reduction during the O₂–H₂ exposure cycle. These results are interpreted by formation of an interfacial Rh–OH species, which permits more effective transfer of hydrogen to ceria, thereby activating oxygen removal from the CeO₂.

Acknowledgments

Research sponsored by the Division of Chemical Sciences, Geosciences, and Biosciences, Office of Basic Energy Sciences, U.S. Department of Energy, under Contract DE-AC05-00OR22725 with Oak Ridge National Laboratory, managed and operated by UT-Battelle, LLC. The authors acknowledge contributions from D.R. Mullins.

References

- [1] H.C. Yao, Y.F.Y. Yao, *J. Catal.* 86 (1984) 254–265.
- [2] A. Trovarelli, *Catal. Rev.-Sci. Eng.* 38 (1996) 439.
- [3] D. Duprez, C. Descorme, in: A. Trovarelli (Ed.), *Catalysis by Ceria and Related Materials*, Imperial Press, London, 2002.
- [4] J. Kaspar, M. Graziani, P. Fornasiero, in: K.A. Gschneidner, L. Eyring (Eds.), in: *Handbook on the Physics and Chemistry of Rare Earths*, vol. 29, Elsevier, Amsterdam, 2000, pp. 159–267.
- [5] B.I. Whittington, C.J. Jiang, D.L. Trimm, *Catal. Today* 26 (1995) 41–45.
- [6] T. Bunluesin, R.J. Gorte, G.W. Graham, *Appl. Catal. B* 15 (1998) 107–114.
- [7] X. Wang, R.J. Gorte, J.P. Wagner, *J. Catal.* 212 (2002) 225–230.
- [8] J.M. Zalc, V. Sokolovskii, D.G. Löffler, *J. Catal.* 206 (2002) 169–171.
- [9] S.J. Schmieg, D.N. Belton, *Appl. Catal. B* 6 (1995) 127.
- [10] J. El-Fallah, S. Boujana, H. Dexpert, A. Kiennemann, J. Majerus, O. Touret, F.F. Villain, F. Le Normand, *J. Phys. Chem.* 98 (1994) 5522–5533.
- [11] S.H. Overbury, D.R. Huntley, D.R. Mullins, G.N. Glavee, *Catal. Lett.* 51 (1998) 133–138.
- [12] G.S. Zafiris, R.J. Gorte, *J. Catal.* 143 (1993) 86–91.
- [13] T. Bunluesin, E.S. Putna, R.J. Gorte, *Catal. Lett.* 41 (1996) 1–5.
- [14] T. Bunluesin, H. Cordatos, R.J. Gorte, *J. Catal.* 157 (1995) 222–226.
- [15] C. De Leitenburg, A. Trovarelli, J. Kaspar, *J. Catal.* 98 (1997) 166.
- [16] D. Terribile, A. Trovarelli, C. De Leitenburg, G. Dolcetti, J. Llorca, *Chem. Mater.* (1997).
- [17] G. Wrobel, C. Lamonier, A. Bergeret, R. Frety, L. Tournayan, O. Touret, *J. Chem. Soc., Faraday Trans.* 92 (1996) 2001.
- [18] Y. Zhang, A. Andersson, M. Muhammed, *Appl. Catal. B* 6 (1995) 325.
- [19] B. Harrison, A.F. Diwell, C. Hallet, *Platinum Met. Rev.* 32 (1988) 73.
- [20] J. Stubenrauch, J.M. Vohs, *J. Catal.* 159 (1996) 50–57.
- [21] L. Kundakovic, D.R. Mullins, S.H. Overbury, *Surf. Sci.* 457 (2000) 51–62.
- [22] H. Cordatos, R.J. Gorte, *J. Catal.* 159 (1996) 112–118.
- [23] H. Cordatos, T. Bunluesin, J. Stubenrauch, J.M. Vohs, R.J. Gorte, *J. Phys. Chem.* 100 (1996) 785–789.
- [24] H. Cordatos, D. Ford, R.J. Gorte, *J. Phys. Chem.* 100 (1996) 18128–18132.

- [25] D.R. Mullins, S.H. Overbury, D.R. Huntley, *Surf. Sci.* 409 (1998) 307–319.
- [26] D.R. Mullins, P.V. Radulovic, S.H. Overbury, *Surf. Sci.* 429 (1999) 186–198.
- [27] J. Stubenrauch, J.M. Vohs, *Catal. Lett.* 47 (1997) 21–25.
- [28] C.T. Campbell, *Surf. Sci. Rep.* 27 (1997) 1–111.
- [29] K. Kato, Y. Abe, M. Kawamura, K. Sasaki, *Jpn. J. Appl. Phys.* 40 (2001) 2399.
- [30] Y. Okamoto, N. Okamoto, N. Ishida, T. Imanata, S. Teranishi, *J. Catal.* 58 (1979) 82.
- [31] J.J. Yeh, I. Lilindau, *Atomic Data and Nuclear Data Tables* 32 (1985) 9.
- [32] J. Soria, A. Martinez-Arias, J.C. Conesa, *J. Chem. Soc., Faraday Trans.* 91 (1995) 1669–1678.
- [33] J.L. d'Itri, V.V. Pushkarev, V.I. Kovalchuk, *Abstr. Pap. Am. Chem. Soc.* 223 (2002) U24–U25.
- [34] J.T. Yates, P.A. Thiel, W.H. Weinberg, *Surf. Sci.* 82 (1975) 45–68.
- [35] B.A. Gurney, W. Ho, *J. Chem. Phys.* 87 (1987) 5562–5577.
- [36] L. Gregoratti, A. Baraldi, V.R. Dhank, G. Comelli, M. Kiskinova, R. Rosei, *Surf. Sci.* 340 (1995) 205–214.